

Particle Motion in Rapidly Oscillating Potentials: The Role of the Potential's Initial Phase

A. Ridinger and N. Davidson.

Department of Physics of Complex Systems, Weizmann Institute of Science, Rehovot 76100, Israel

(Dated: December 26, 2019)

Rapidly oscillating potentials with a vanishing time average have been used for a long time to trap charged particles in source-free regions. It is well-known that the motion of a particle inside such a potential can be approximately described by a time independent effective potential, which does not depend upon the initial phase of the oscillating potential. Here we show that the motion of a particle and its trapping condition significantly depend upon this initial phase for arbitrarily high frequencies. We solve this apparent contradiction by showing that a particle's motion is not determined by the effective potential alone, but also by a transformation of its initial conditions. This transformation is shown to significantly depend on the initial phase and on the particle's initial conditions for arbitrarily high frequencies. We give a theoretical description of this novel phenomenon which we then confirm by numerical simulations. Further, we demonstrate that it offers new ways to manipulate the dynamics of particles which are trapped by rapidly oscillating potentials. Finally, we propose a simple experiment to verify the theoretical findings of this work.

I. INTRODUCTION

The theoretical study of the dynamics of a particle moving inside a rapidly oscillating potential has been an active field of research for the past 50 years [1, 2, 3, 4, 5, 6, 7, 8, 9, 10]. In 1951, P.L. Kapitza showed that rapidly oscillating potentials can have a stabilizing effect on dynamical systems [1], which he demonstrated utilizing an inverted pendulum whose suspension point was forced to oscillate vertically. For high enough frequencies and large enough amplitudes of this oscillation the upwards position of the pendulum becomes stable. Kapitza showed that the pendulum feels an *effective* potential that has a local minimum at the pendulum's upwards position and thus imparts stability upon it. This phenomenon has since been termed "dynamic stabilization". In 1958, W. Paul used the principle of dynamic stabilization to trap charged ions by alternating electric fields [11]. Ions trapped within a Paul trap have and continue to be used in the development of frequency standards, other fundamental measures [12] and quantum information [13].

In order to grasp all the possible applications that are offered by atoms which are trapped by rapidly oscillating potentials, a descriptive theory of their dynamics is indispensable. For the motion of ions inside a Paul trap such a theory is given by Mathieu's theory, which provides the exact solution of the ion's classical equations of motion in terms of the tabulated Mathieu functions [11, 14, 15]. However, this theory is restricted to potentials of harmonic shape which are oscillated sinusoidally only. Besides this, Mathieu's theory does not raise intuition regarding the atom's dynamics hindering the discovery of new phenomena. For these purposes, Kapitza's theory of the effective potential has thus far been suitable, sufficiently explaining the stabilization of the inverted pendulum [1]. This theory has since been generalized to arbitrary oscillating potentials [2, 10] and extended to

quantum mechanics [8, 9, 10]. The effective potential theory gives an approximation of the particle's motion which is valid for large frequencies of the potential's oscillation.

In this paper we investigate the effect of the initial phase of arbitrary rapidly oscillating potentials on the motion of a particle which moves inside them. According to the effective potential theory, a particle inside such a potential behaves as if it was exposed to a time independent effective potential, which does not depend on the oscillating potential's initial phase. However, here we show, that for given initial conditions of the particle, its motion is not exclusively determined by this effective potential, but also by a transformation of the particle's initial conditions. We explicitly derive this transformation and show that it significantly depends on the potential's initial phase, resulting in a particle motion which significantly depends on the initial phase even for arbitrarily high frequencies of the potential's oscillation. We further verify this phenomenon by numerical simulations considering two simple examples, a particle moving inside an oscillating Gaussian-shaped potential and inside an oscillating parabola-shaped potential. This phenomenon is clearly manifested in the particle's stability region (i.e. the region in phase space that contains all initial conditions of the particle leading to subsequent trapping by the oscillating potential) for which we derive an explicit formula, which we also verify by numerical simulations.

The phenomenon of the dependence of the particle's motion on the potential's initial phase offers the possibility to manipulate the trapped particles in a simple and controlled manner. For example, modification of the oscillating potential's phase at some point in time by a discrete value (inducing a phase hop) results in a change of the trapped particle's average energy. We explicitly calculate this phase hop induced change in energy and show that it is significant for arbitrarily high frequencies of the potential's oscillation.

Throughout the paper we use one dimensional formalism, but the results presented here can be directly applied to two and three dimensions in cases where the motion is separable [2]. For high dimensional oscillating potentials where the particle's motion is not separable and in particular chaotic, new phenomena may occur that are not discussed here [16].

II. PARTICLE MOTION IN A RAPIDLY OSCILLATING POTENTIAL

Newton's equation for a particle with mass m that is moving inside a one-dimensional rapidly oscillating potential $V(x, t)$ can be written as

$$m\ddot{x} = -V'(x, t) = -V'_0(x) - V'_1(x)f(\omega t + \varphi), \quad (1)$$

where $V_0(x)$ describes the time average part of $V(x, t)$ and $V_1(x)$ its oscillating part and $f(\omega t)$ its time modulation function which has period 2π , unity amplitude and vanishing time average over one period. The frequency of the potential's oscillation is denoted by ω . φ is the initial phase of the oscillating potential $V(x, t)$. Derivatives with respect to coordinates are denoted by primes and with respect to time by dots. The average over one period of oscillation (period-average) of a 2π -periodic function $g(\tau)$ is denoted by a bar: $\bar{g} \equiv \frac{1}{2\pi} \int_0^{2\pi} g(\tau) d\tau$. If the frequency ω is very large compared to the other time scales of the system, the time dependent equation of motion (1) can be replaced by a time independent *effective* equation of motion that yields the period-averaged motion of the particle [10]. This effective equation of motion can be obtained by separating the motion $x(t)$ of the particle into a sum of a slow part $X(t)$, which depends on the slow time t , and a fast part $\xi(\tau)$, which depends on the fast time $\tau \equiv \omega t$:

$$x(t) = X(t) + \xi(\tau). \quad (2)$$

$X(t)$ and $\xi(\tau)$ will be referred to as the slow and the fast motion, respectively. For large frequencies ω , the amplitude of the fast motion ξ can be assumed to be small, since due to its inertia, the particle does not have the time to react to the force which is induced by the oscillating potential, before this force changes sign. Thus, for large frequencies, ξ can be expanded in powers of the inverse frequency: $\xi(\tau) = \sum_{i=1}^{\infty} \frac{1}{\omega^i} \xi_i(\tau)$. Requiring that on the fast time scale τ , the fast motion ξ is periodic with a vanishing period-average, the particle's period-averaged motion $\bar{x}(t)$ is given by the slow motion, $\bar{x}(t) = X(t)$. Further requiring that the definition of ξ leads to a time independent equation of motion for the slow motion $X(t)$, uniquely defines ξ and yields the effective equation of motion for $X(t)$. This calculation is presented in reference [10]. Its results in the leading order in ω^{-1} are the explicit expression of ξ ,

$$\xi(\tau, X, \varphi) = -\frac{1}{m\omega^2} V'_1(X) \int^{(2)\tau} [f(\tau + \varphi)], \quad (3)$$

and the effective equation of motion

$$m\ddot{X} = -V'_{\text{eff}}(X) \quad (4)$$

with the effective potential

$$V_{\text{eff}}(X) = V_0(X) + \frac{1}{2m\omega^2} V'_1(X)^2 \overline{\left(\int^\tau [f(\tau)] \right)^2}. \quad (5)$$

$\int^\tau [f(\tau)] \equiv \sum_{n \neq 0} \frac{1}{in} f_n e^{in\tau}$ is the standardized integral [17], which is defined for 2π -periodic functions $f(\tau)$ that have vanishing period-average and whose Fourier expansion is given by $f(\tau) = \sum_{n \neq 0} f_n e^{in\tau}$. According to this definition, the standardized integral is simply the anti-derivative of $f(\tau)$ which has vanishing period-average. Thus, it can be applied repeatedly. Its multiple application (j times) is denoted by $\int^{(j)\tau} [f(\tau)]$ and its evaluation at the point τ_0 by $[\int^\tau [\dots]]_{\tau_0}$.

The effective potential (5) for the slow motion $X(t)$ is independent of φ . Therefore, one might naively expect, that the period-averaged motion $X(t)$ of a particle inside a rapidly oscillating potential is also independent of φ . In order to address this question we first inspect the particle's motion for a given φ . For that matter, we compare both the position $x(t)$ with its period-average $X(t)$ and the velocity $\dot{x}(t)$ with its period-average $\dot{X}(t)$ (For a numerical example see section III, Fig. 2). We restrict ourselves to the physically interesting case of a particle that is trapped by a rapidly oscillating potential with a vanishing time average (i.e. $V_0 \equiv 0$). The position $X(t)$ and the velocity $\dot{X}(t)$ of the period-averaged motion are determined by equation (4). Thus, for the particle to be trapped, the effective potential (5) must have a local minimum. The spatial width of this local minimum determines the spatial confinement of the particle, and is according to (5) independent of ω . Thus, the position $X(t)$ of the trapped particle's slow motion is of the order ω^0 . According to (3), the position $\xi(t)$ of its fast motion is of the order ω^{-2} and therefore in the limit of large ω negligible compared to the position $X(t)$ of its slow motion. This means, that for large ω one can approximate $x(t) = X(t) + \xi(t) \approx X(t)$ (see Fig. 2(a)).

The depth of the effective potential's local minimum determines which kinetic energies the trapped particle can have. It is according to (5) of the order ω^{-2} . Thus, the velocity $\dot{X}(t)$ of the particle's slow motion is of the order ω^{-1} . The velocity $\dot{\xi}(t)$ of its fast motion is given by the derivative of (3) with respect to time,

$$\dot{\xi}(t, \varphi) = -\frac{1}{m\omega} V'_1(x(t)) \left[\int^\tau [f(\tau + \varphi)] \right]_{\tau=\omega t}, \quad (6)$$

which is a term of the order ω^{-1} and thus of the same order than $\dot{X}(t)$. Therefore, the velocity $\dot{\xi}(t)$ of the trapped particle's fast motion is for large ω not negligible compared to the velocity $\dot{X}(t)$ of its slow motion. As a result, even for large ω one cannot approximate $\dot{x}(t) = \dot{X}(t) + \dot{\xi}(t) \approx \dot{X}(t)$ (see Fig. 2(b)).

This observation explains that in order to determine the particle's period-averaged motion with the effective equation of motion (4) for given initial conditions $x(0)$ and $\dot{x}(0)$ one has to perform the initial condition assignment

$$\begin{aligned} X(0) &= x(0) \\ \dot{X}(0) &= \dot{x}(0) - \dot{\xi}(0) \end{aligned} \quad (7)$$

with

$$\dot{\xi}(0) = -\frac{1}{m\omega} V_1'(x(0)) \left[\int_{\tau=0}^{\tau} [f(\tau+\varphi)] \right], \quad (8)$$

whereas the contribution of $\dot{\xi}(0)$ in (7) cannot be neglected.

Expression (8) depends on the term $\left[\int_{\tau=0}^{\tau} [f(\tau+\varphi)] \right]$ which is a function of the initial phase φ of the oscillating potential $V(x, t)$. The initial condition assignment (7) therefore depends on φ , which implies that the resulting period-averaged motion $X(t)$ of the particle also depends on φ (For a numerical example see section III, Fig. 3). Further inspection of expression (8) shows, that it also depends on the initial position $x(0)$ of the particle. This implies that the degree of dependence of the particle's motion on the initial phase is determined by the particle's initial position. In the special case that the term $\left[\int_{\tau=0}^{\tau} [f(\tau+\varphi)] \right]$ vanishes, the initial conditions of the slow motion, $X(0)$, $\dot{X}(0)$, equal the real initial conditions, $x(0)$, $\dot{x}(0)$, such that in this case the motion of the particle is determined by the time independent effective potential (5) alone. Since $\int^{\tau} [f(\tau)]$ is 2π -periodic and has vanishing average, there always exist two phases $\varphi_1, \varphi_2 \in [0, 2\pi]$ for which $\left[\int_{\tau=0}^{\tau} [f(\tau+\varphi_1)] \right]$ and $\left[\int_{\tau=0}^{\tau} [f(\tau+\varphi_2)] \right]$ vanish. Thus, for every given rapidly oscillating potential there exist two phases for which the motion of any particle inside this potential is determined only by its time-independent effective potential.

The significance of the highlighted dependence of a particle's motion on the initial phase is manifested in the particle's stability region (i.e. the region in phase space that contains all initial conditions of the particle leading to subsequent trapping by the oscillating potential). Since the effective potential (5) in equation (4) is time independent, the principle of energy conservation can be invoked for its calculation. For a trapping effective potential we define $X = 0$ as the position of the bottom of the trap and $X = L$ as the position of the trap boundary. Thus, the initial conditions $X(0)$, $\dot{X}(0)$ belong to the stability region if they obey the inequality

$$\frac{1}{2} m \dot{X}(0)^2 + V_{\text{eff}}(X(0)) \leq V_{\text{eff}}(L). \quad (9)$$

Substituting (7), solving for $\dot{x}(0)$ and neglecting terms of higher order than ω^{-1} yields

$$\begin{aligned} \dot{x}(0) &\leq -\frac{1}{m\omega} V_1'(x(0)) \left[\int_{\tau=0}^{\tau} [f(\tau+\varphi)] \right] \\ &\pm \frac{1}{m\omega} \sqrt{\left(\int_{\tau=0}^{\tau} [f(\tau)] \right)^2} \sqrt{V_1'(L)^2 - V_1'(x(0))^2}, \end{aligned} \quad (10)$$

which defines the stability region for large ω . The right hand side of (10) consists of a phase dependent and a phase independent term which are both of the same order, such that the stability region significantly depends on the phase φ for arbitrarily large ω . In section III, we explicitly calculate the stability region for different φ for two numerical examples.

In the previous paragraphs we showed, that due to the dependence of the fast motion's initial velocity $\dot{\xi}(0)$ on the initial phase φ and due to the significant coupling between the particle's slow motion $X(t)$ and $\dot{\xi}(0)$, the particle's slow motion $X(t)$ is significantly coupled to φ . φ can therefore be used to manipulate the particle's motion. For example, if φ is modified instantaneously by a discrete value $\Delta\varphi$ (a phase hop), the position $X(t)$ of the particle's slow motion will, on the time scale of the slow motion, change in a non-smooth manner and the velocity $\dot{X}(t)$ will, on this time scale, change non-continuously by a discrete value, $\Delta\dot{X}$. According to (7), this change is given by

$$\Delta\dot{X}(t_{\text{ph}}) = \frac{1}{m\omega} V_1'(X(t_{\text{ph}})) \cdot \tilde{\Delta}, \quad (11)$$

with

$$\tilde{\Delta} = \left[\int_{\tau=\omega t_{\text{ph}}}^{\tau} [f(\tau+\varphi+\Delta\varphi)] - \int_{\tau=\omega t_{\text{ph}}}^{\tau} [f(\tau+\varphi)] \right], \quad (12)$$

where t_{ph} denotes the time at which the phase hop is induced. This change in the velocity of the particle's slow motion results in an instantaneous change ΔE (on the slow time scale) of the period-averaged total energy E of the particle, which is given by

$$\Delta E(t_{\text{ph}}) = m \dot{X}(t_{\text{ph}}) \Delta\dot{X}(t_{\text{ph}}) + \frac{1}{2} m (\Delta\dot{X}(t_{\text{ph}}))^2, \quad (13)$$

where $\dot{X}(t_{\text{ph}})$ denotes the velocity of the slow motion right before the phase hop. As can be seen from formulas (11) and (13), $\Delta E(t_{\text{ph}})$ is of the same order (ω^{-2}) than E . Thus, the period-averaged total energy E of a trapped particle can be significantly manipulated by a phase hop for arbitrarily large ω . As an example, we calculate ΔE for the special case $f(\tau+\varphi) = \cos(\tau+\varphi)$, and assume that the phase hop is induced at the time $t = t_{\text{ph}}$ for which $\int_{\tau=\omega t_{\text{ph}}}^{\tau} [\cos(\tau+\varphi)] = 0$ (which is the case twice each period of the fast motion), and for which the kinetic energy of the slow motion equals three quarters of the total period-averaged energy, that is $\frac{1}{2} m \dot{X}(t_{\text{ph}})^2 = \frac{3}{4} E$ (this is the case four times each period of the slow motion). Due to energy conservation of the slow motion, it is $V_{\text{eff}}(X(t_{\text{ph}})) \equiv \frac{1}{4m\omega^2} V_1'(X(t_{\text{ph}}))^2 = \frac{1}{4} E$. We further assume that the size of the phase hop $\Delta\varphi$ equals $\frac{\pi}{2}$, such that $\int_{\tau=\omega t_{\text{ph}}}^{\tau} [\cos(\tau+\varphi+\Delta\varphi)] = 1$. Then

$$\begin{aligned} \Delta E(t_{\text{ph}}) &= m \dot{X}(t_{\text{ph}}) \frac{1}{m\omega} V_1'(X(t_{\text{ph}})) + \frac{1}{2m\omega^2} V_1'(X(t_{\text{ph}}))^2 \\ &= \left(\frac{1}{2} \pm \sqrt{\frac{3}{2}} \right) E, \end{aligned} \quad (14)$$

where the minus sign holds for $\dot{X}(t_{\text{ph}}) V'_1(X(t_{\text{ph}})) < 0$ and the plus sign for $\dot{X}(t_{\text{ph}}) V'_1(X(t_{\text{ph}})) > 0$. ΔE is therefore independent of ω (for large ω) and proportional to E , so that the relative change, $\frac{\Delta E}{E}$, is independent of E . It is therefore always possible to take away more than two thirds of a trapped particle's energy or to give more than five thirds of its energy by inducing a phase hop (For numerical examples see section III, Fig. 4 and Fig. 5). In section IV, we propose an experiment which may verify this conclusion.

III. NUMERICAL EXAMPLES

In this section we consider two simple examples in order to demonstrate the phenomenon found in the previous section and to compare the derived analytical predictions to results of numerical simulations. The first example to be considered is a particle moving inside an oscillating Gaussian-shaped potential with a vanishing time average of the form

$$V^G(x, t) = \gamma \exp\left(-\frac{2x^2}{w_0^2}\right) \cos(\omega t + \varphi) \quad (15)$$

which is illustrated in Fig. 1(a). Potential (15) defines

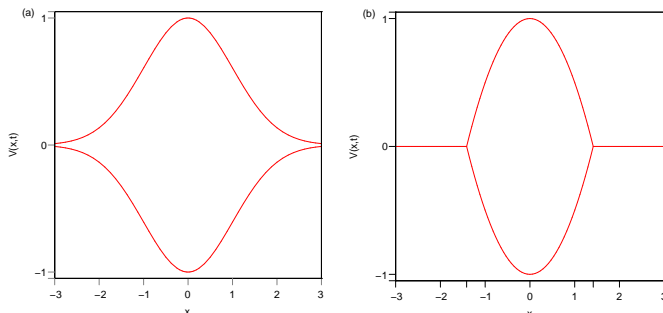


FIG. 1: (color online) (a) Oscillating Gaussian-shaped potential (15), (b) oscillating clipped parabola-shaped potential (18). Units: $V(x, t)$ in γ , x in $0.5 w_0$.

two time scales: the time scale associated with the frequency ω of the potential's oscillation and the time scale associated with the oscillation frequency ω_{osc} of a low energy particle in the minimum instantaneous potential. The theory which was derived in section II is valid for large frequencies ω compared to the frequencies which are associated with the other time scales of the system. In the following we therefore consider the regime $\omega \gg \omega_{\text{osc}}$.

In the last section we showed theoretically, that the position of a trapped particle can be approximated by the position of its slow motion and that its velocity cannot be approximated by the velocity of its slow motion. To verify this, we numerically simulate a particle's trajectory in position and velocity space and compare it to its period-average. This is done by numerically integrating

the time dependent Newton equation

$$m\ddot{x} = \frac{4\gamma}{w_0^2} x \exp\left(-\frac{2x^2}{w_0^2}\right) \cos(\omega t + \varphi). \quad (16)$$

The results are shown in Fig. 2. In the figure one can

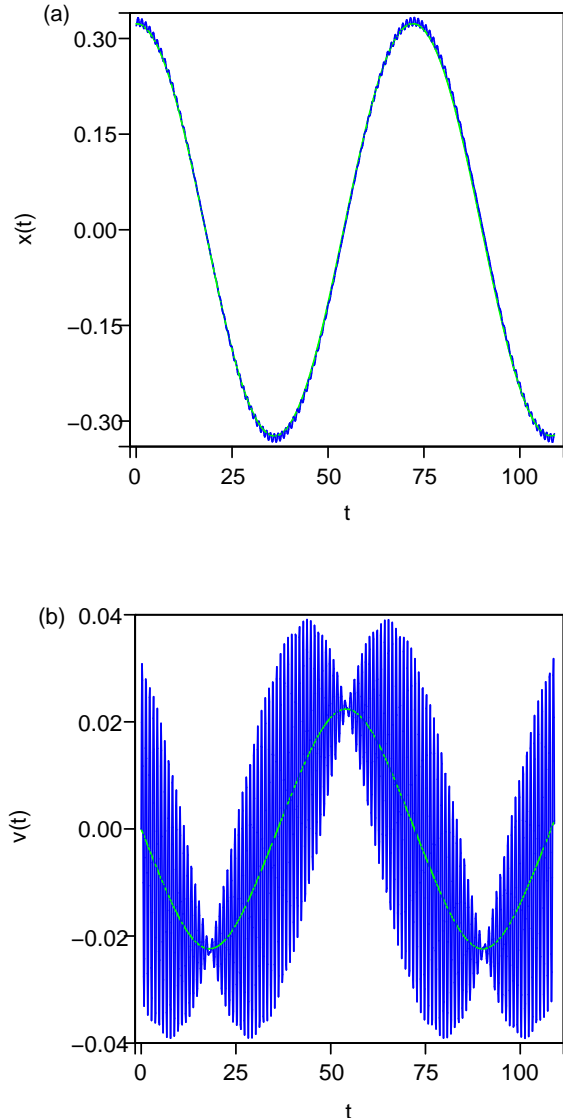


FIG. 2: (color online) Trajectory of a particle inside the oscillating Gaussian-shaped potential (15) obtained from numerical simulations (a) in position space, (b) in velocity space. Blue curve: real trajectory, green curve: period-averaged trajectory. Units: $x(t)$ in $0.5 w_0$, $v(t) \equiv \dot{x}(t)$ in $\sqrt{2\gamma/m}$, t in $2\pi/\omega$. Parameters: $\omega = 7 \omega_{\text{osc}}$, $\varphi = 0$. Initial conditions: $x(0) = 0.32 w_0$, $\dot{x}(0) = 0$. The real and period-averaged trajectory are nearly identical in position space but largely differ in velocity space.

clearly see that the trajectory in position space (Fig. 2(a), blue curve) is well described by its period-average (Fig. 2(a), green curve), whereas in velocity space (Fig. 2(b))

this is not the case. Additional numerical simulations showed that this result does not change when ω is increased, in agreement with the derived theory.

In section II we showed, that the significant difference between the particle's velocity and its period-average (Fig. 2(b)) leads to a dependence of the particle's motion on the initial phase φ of the oscillating potential. To verify this conclusion, we numerically simulate the particle's trajectory in position space for different φ for a given frequency ω and given initial conditions of the particle. The result is shown in Fig. 3. The charted trajectories

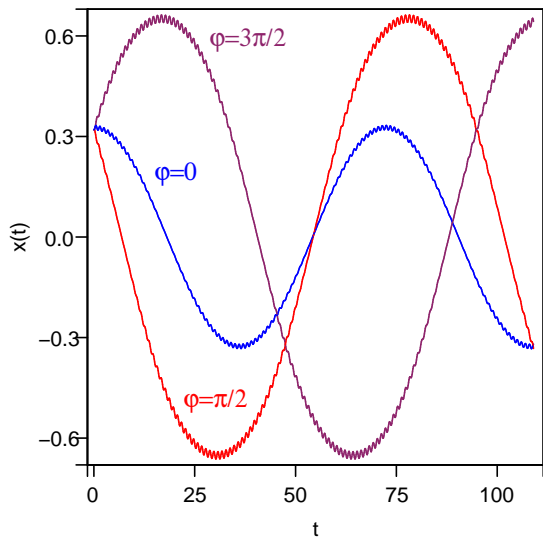


FIG. 3: (color online) Trajectory in position space of a particle inside the oscillating Gaussian-shaped potential (15) for different φ , obtained from numerical simulations. Units: $x(t)$ in $0.5 w_0$, t in $2\pi/\omega$. Parameters: $\omega = 7\omega_{\text{osc}}$ and $\varphi = 0$ (blue curve), $\varphi = \frac{\pi}{2}$ (red curve) and $\varphi = \frac{3\pi}{2}$ (purple curve). Initial conditions: $x(0) = 0.32 w_0$, $\dot{x}(0) = 0$. The shown trajectories are nearly indistinguishable from their theoretical predictions calculated from (5) and (7), which are therefore not shown in the figure.

appreciably differ from each other, as predicted by the derived theory. On the slow time scale they have different phases and different amplitudes. Figure 3 shows as well, that all trajectories appear to be generated from the same time independent effective potential. Since the trajectories for different φ are not the same although their initial conditions are, this verifies that the trajectories are determined in addition by a transformation of their initial conditions which depends on φ . In section II we derived an analytical expression of this transformation (7). Using this formula and formula (5) for the effective potential one can exactly obtain the period-average of the trajectories shown in Fig. 3, which were not charted so not to constrain the clarity of the figure (The derived transformation (7) is numerically verified quantitatively through the calculation of the particle's stability region, as shown below).

Another result of section II to be verified by numer-

ical simulations is the prediction of the particle's motion when phase hops in the oscillating potential's time modulation function are induced. Figure 4 shows the numerically simulated trajectory of the particle for a phase hop of size $\Delta\varphi = \frac{\pi}{2}$ induced at the time $t = t_{\text{ph}}$ for which $\int^\tau [\cos(\tau + \varphi)]_{\tau=\omega t_{\text{ph}}} = 0$, and for which $\frac{1}{2}m\dot{X}(t_{\text{ph}})^2 \approx \frac{3}{4}E$. In agreement with the analytical for-

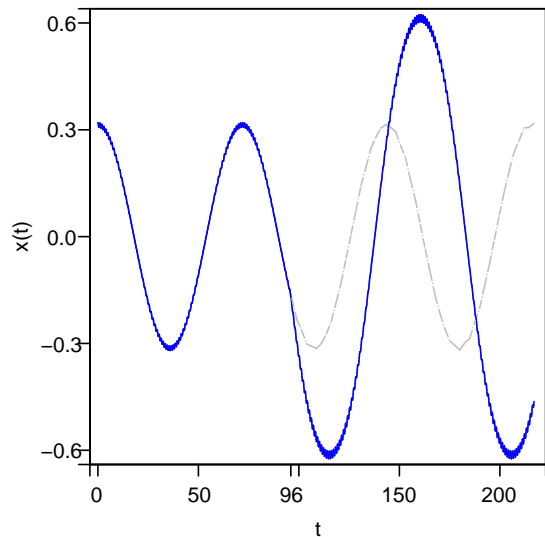


FIG. 4: (color online) Trajectory in position space of a particle inside the oscillating Gaussian-shaped potential (15) when a phase hop is induced, obtained from numerical simulations. Blue solid curve: real trajectory, grey dot-dashed curve: imaginary continuation of trajectory when no phase hop were induced. Units: $x(t)$ in $0.5 w_0$, t in $2\pi/\omega$. Parameters: $\omega = 7\omega_{\text{osc}}$, $\varphi = \pi$, time of phase hop $t_{\text{ph}} = 96 \cdot \frac{2\pi}{\omega}$ and phase hop size $\Delta\varphi = \frac{\pi}{2}$. Initial conditions: $x(0) = 0.32 w_0$, $\dot{x}(0) = 0$. The phase hop changes the particle's total energy by a factor of approximately 2.7 in agreement with formula (14). The shown trajectory is nearly indistinguishable from its theoretical prediction (not shown) calculated from (5) and (7).

mula (14), the period-averaged energy of the particle in Fig. 4 indeed changes by a factor of approximately 2.7. Using the derived analytical formulas (5) and (7) one can exactly obtain the period-average of the trajectory shown in Fig. 4, whereas the part of the trajectory after the phase hop is obtained from these formulas by assigning the time of the phase hop to the initial time. The result was not charted so not to constrain the clarity of the figure. Figure 5 shows the numerically simulated trajectory of the particle when several phase hops are induced. The size of the phase hops was always $\Delta\varphi = \frac{\pi}{2}$ and the moments of the phase hops $t_i = t_{\text{ph}}^{(i)}$ were chosen such that the particle loses energy through each phase hop and that $\int^\tau [\cos(\tau + \varphi)]_{\tau=\omega t_{\text{ph}}^{(i)}} = 0$ and $\frac{1}{2}m\dot{X}(t_{\text{ph}}^{(i)})^2 \approx \frac{3}{4}E(t_{\text{ph}}^{(i)})$, whereas $E(t_{\text{ph}}^{(i)})$ denotes the particle's total energy right before the i -th phase hop. In agreement with the analytical formula (14), the period-averaged energy of the

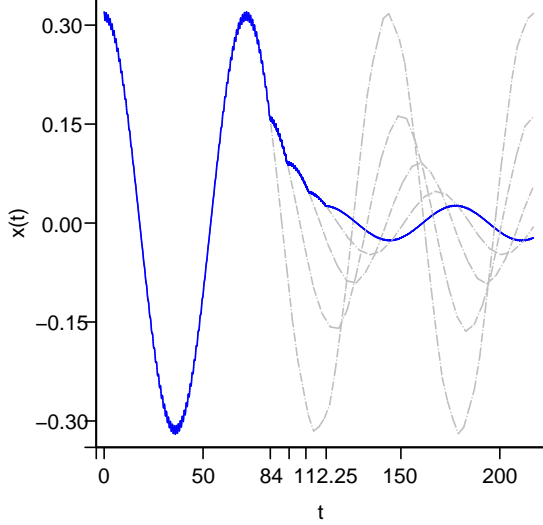


FIG. 5: (color online) Trajectory in position space of a particle inside the oscillating Gaussian-shaped potential (15) when a series of 4 phase hops is induced, obtained from numerical simulations. Blue solid curve: real trajectory, grey dot-dashed curves: imaginary continuations of trajectory when the phase hops were not induced. Units: $x(t)$ in $0.5 w_0$, t in $2\pi/\omega$. Parameters: $\omega = 7\omega_{\text{osc}}$, $\varphi = \pi$, times of phase hops $t_{\text{ph}}^{(1)} = 84 \cdot \frac{2\pi}{\omega}$, $t_{\text{ph}}^{(2)} = 92.75 \cdot \frac{2\pi}{\omega}$, $t_{\text{ph}}^{(3)} = 103.5 \cdot \frac{2\pi}{\omega}$, $t_{\text{ph}}^{(4)} = 112.25 \cdot \frac{2\pi}{\omega}$, and phase hop size $\Delta\varphi = \frac{\pi}{2}$. Initial conditions: $x(0) = 0.32 w_0$, $\dot{x}(0) = 0$. The phase hops change the particle's total energy by a factor of approximately $1/170$ in agreement with formula (14). The shown trajectory is nearly indistinguishable from its theoretical prediction (not shown) calculated from (5) and (7).

particle in Fig. 5 changes in total by a factor of approximately $\frac{1}{170}$. Figure 5 demonstrates that this substantial change in energy can be achieved even when the phase hops are induced very quickly one after another (within a fraction of the period of the particle's slow motion). Using the derived analytical formulas (5) and (7) one can exactly obtain the period-average of the trajectory shown in Fig. 5, which is again not charted so not to constrain the clarity of the figure.

The last theoretical prediction of section II that is to be verified by numerical simulations in the following is the derived analytical formula (10) for the stability region. According to this formula, the stability region of the particle inside the oscillating Gaussian-shaped potential (15) is given by

$$\dot{x}^G \leq -\frac{1}{m\omega} \frac{4\gamma}{w_0^2} x \exp\left(-\frac{2x^2}{w_0^2}\right) \sin \varphi \\ \pm \frac{1}{m\omega} \frac{\sqrt{8}\gamma}{w_0^2} \sqrt{\frac{w_0^2}{4} \exp(-1) - x^2 \exp\left(-\frac{4x^2}{w_0^2}\right)}. \quad (17)$$

A graph of this analytical prediction of the stability region for different φ is shown in Fig. 6 (solid curves). Before comparing this analytical prediction to the results of

numerical simulations, we first discuss it separately. In

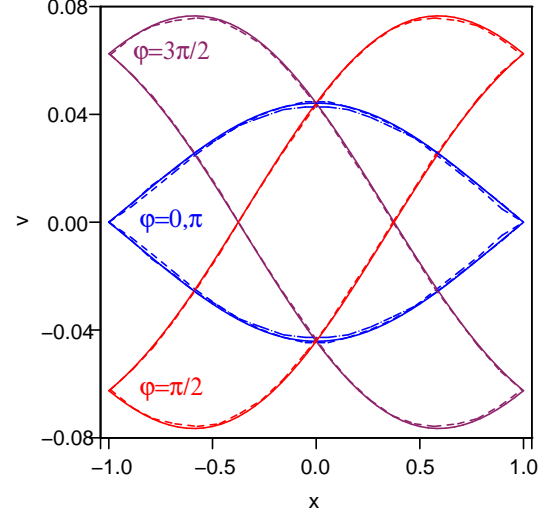


FIG. 6: (color online) Stability region for a particle inside the oscillating Gaussian-shaped potential (15) for different phases φ and for $\omega = 7\omega_{\text{osc}}$. Solid curves: analytical prediction (17) for $\varphi = 0$ (blue), $\varphi = \frac{\pi}{2}$ (red), $\varphi = \pi$ (also blue), and $\varphi = \frac{3\pi}{2}$ (purple). Dashed curves: results of numerical simulations for $\varphi = 0$ (blue), $\varphi = \frac{\pi}{2}$ (red), and $\varphi = \frac{3\pi}{2}$ (purple). Dot-dashed curve: for $\varphi = \pi$ (blue). Units: $v \equiv \dot{x}$ in $\sqrt{2\gamma/m}$, x in $0.5 w_0$.

Fig. 6 one can clearly see, that the analytically predicted stability regions for different φ significantly differ from each other. For the initial phases $\varphi = 0$ and $\varphi = \pi$ the stability regions are identical and axially symmetrical to the coordinate axes. For the phases $\varphi = \frac{\pi}{2}$ and $\varphi = \frac{3\pi}{2}$ the stability regions are not axially symmetrical to the coordinate axes and particularly not to the position axis. This demonstrates, that the motion of the particle cannot be determined by a time independent effective potential alone, since the stability region of any time independent potential is due to energy conservation axially symmetric to the position axis. Compared to the stability regions of the phases $\varphi = 0$ and $\varphi = \pi$, those of the phases $\varphi = \frac{\pi}{2}$ and $\varphi = \frac{3\pi}{2}$ further look distorted and rotated around the origin. One can see, that the area of the stability region is independent of the initial phase φ , which immediately emerges from formula (10). The overlap of two stability regions of different φ in units of their total area, however, depends on the initial phase of the respective overlapping stability regions, but is according to (10) independent of ω . The spatial width of the stability region is independent of the initial phase φ and according to (10) also independent of ω . As a last observation it is clear that the boundaries of all stability regions intersect at $x = 0$, meaning that the escape velocity of the particle that is initially situated at $x = 0$ is the same regardless of the initial phase φ . This is, because for $x(0) = 0$ the initial condition assignment (7) is independent of φ , since it is $V_1'(0) = 0$.

We now compare the analytical prediction for the sta-

bility region (17) to results of numerical simulations, which are shown as dashed and dot-dashed curves in Fig. 6. The numerical simulations were performed as follows: First, the particle's phase space was discretized into a grid of equally spaced points, each of which defining possible initial conditions of the particle. Then, the time dependent Newton equation (16) was integrated numerically for each of these points. Thus, all the points, which generated a trajectory that stayed within a prespecified spatial region within a prespecified *large* time, were defined as points of the stability region. The prespecified values for the spatial region ($|x| \lesssim \frac{w_0}{2}$) and the *large* time ($t \approx 200 \cdot \frac{2\pi}{\omega}$) were chosen such that further increase in these values did not change the result appreciably. The step size was chosen to be $\Delta t = \frac{1}{100} \cdot \frac{2\pi}{\omega}$, since further decrease of the step size did not alter the results appreciably. Figure 6 shows a very good agreement between theory and simulations. Additional simulations showed, that this agreement increases when ω is increased, as expected from the theory.

So far we have considered a particle moving inside the oscillating Gaussian-shaped potential (15). Another example to be considered in the following, a particle moving inside an oscillating clipped parabola-shaped potential with a vanishing time average of the form

$$V^{\text{cp}}(x, t) = V_1(x) \cos(\omega t + \varphi) \quad (18)$$

with

$$V_1(x) = \begin{cases} -kx^2 + kL^2 & \text{for } |x| \leq L, \\ 0 & \text{else.} \end{cases} \quad (19)$$

which is illustrated in Fig. 1(b). This is a problem able to be solved exactly, because the particle's time dependent Newton equation

$$m\ddot{x} = \begin{cases} 2kx \cos(\omega t + \varphi) & \text{for } |x| \leq L, \\ 0 & \text{else.} \end{cases} \quad (20)$$

is for $|x| \leq L$ equivalent to the homogeneous Mathieu equation, whose solution is given by a linear combination of the Mathieu functions [11, 14, 15], and for $|x| \geq L$ it is equivalent to the trivial differential equation $\ddot{x} = 0$ of free motion. Therefore, the considered example allows for a comparison between the theory that was derived in section II and the Mathieu theory. We choose $L = \frac{w_0}{\sqrt{2}}$ and $k = \frac{\gamma}{L^2}$ so that in (18) the reference frequency $\omega_{\text{osc}} = \sqrt{\frac{4\gamma}{mw_0^2}}$ as well as the maximum instantaneous potential depth γ are the same as in (15). In the following we calculate the particle's stability region - once by using the derived analytical formula (10) and once by applying Mathieu's theory. Formula (10) yields

$$\dot{x}^{\text{cp}} \leq -\frac{1}{m\omega} \frac{4\gamma}{w_0^2} x \sin(\varphi) \pm \frac{1}{m\omega} \frac{2\sqrt{2}\gamma}{w_0^2} \sqrt{\frac{w_0^2}{2} - x^2}. \quad (21)$$

A graph of this analytical prediction of the stability region is shown in Fig. 7 (solid curves) for different φ . Figure 7 also shows the results obtained from Mathieu's theory (dashed and dot-dashed curves). It can be seen that

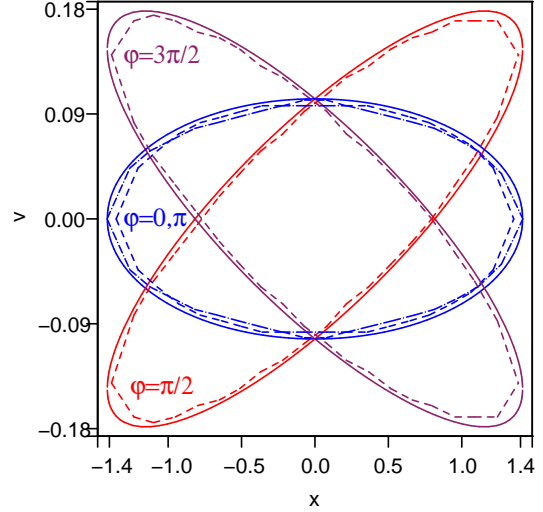


FIG. 7: (color online) Stability region for a particle inside the oscillating clipped parabola-shaped potential (18) for different phases φ and for $\omega = 7\omega_{\text{osc}}$. Solid curves: analytical prediction of derived formula (21) for $\varphi = 0$ (blue), $\varphi = \frac{\pi}{2}$ (red), $\varphi = \pi$ (also blue), and $\varphi = \frac{3\pi}{2}$ (purple). Dashed curves: results of Mathieu's theory for $\varphi = 0$ (blue), $\varphi = \frac{\pi}{2}$ (red), and $\varphi = \frac{3\pi}{2}$ (purple). Dot-dashed curve: for $\varphi = \pi$ (blue). Units: $v \equiv \dot{x}$ in $\sqrt{2\gamma/m}$, x in $0.5w_0$.

the stability regions of the particle have the shape of an ellipse. Figure 7 shows a very good agreement of our derived theory and the Mathieu theory. In order to confirm the accuracy of the numerical simulations which we performed for the oscillating Gaussian-shaped potential in the previous paragraph, we repeated these simulations for the parabola-shaped potential finding that the obtained results were identical to those obtained from Mathieu's theory. All main results which we demonstrated for the oscillating Gaussian-shaped potential were found also for the oscillating parabola-shaped potential.

IV. PROPOSAL OF AN EXPERIMENT

In this section, we propose an experiment to verify our theoretical results. Consider an ensemble of atoms that is trapped inside a rapidly oscillating potential with a vanishing time average, whose amplitude is chosen such that the ensemble uniformly fills its stability region. Hence, the fraction of atoms which remain trapped after a phase hop of the oscillating potential is induced, is equal to the mutual overlap of the stability region with the initial time given by the time right before the phase hop and the stability region with the initial time given by the time right

after the phase hop. This overlap is exactly determined by formula (10). It is a function of the time t_{ph} when the phase hop is induced and of the size $\Delta\varphi$ of the phase hop. Figure 8 shows this overlap for a two-dimensional oscillating Gaussian-shaped potential. One can see that

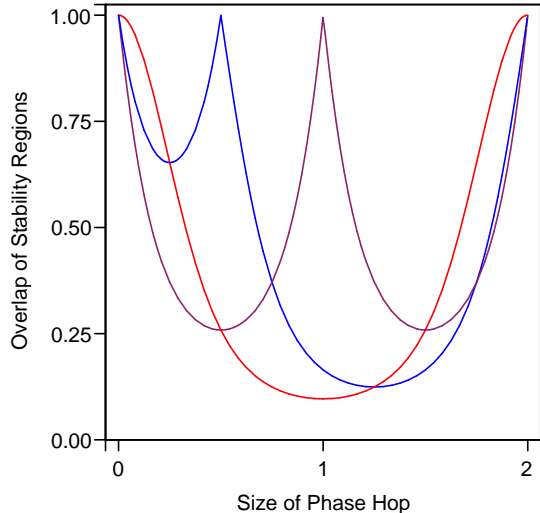


FIG. 8: (color online) Overlap of the stability region of initial phase φ with the stability region of initial phase $\varphi + \Delta\varphi$ for different t_{ph} as a function of $\Delta\varphi$ obtained from the two dimensional extension of formula (10) for an oscillating Gaussian-shaped potential. Red curve: $(\omega t_{\text{ph}} + \varphi) \bmod 2\pi = \frac{\pi}{2}$, blue curve: $(\omega t_{\text{ph}} + \varphi) \bmod 2\pi = \frac{3\pi}{4}$, maroon curve: $(\omega t_{\text{ph}} + \varphi) \bmod 2\pi = \pi$. The overlap of the stability regions is given in units of their total volume and the size $\Delta\varphi$ of the phase hop in units of π .

regardless of t_{ph} , at least 60% of the atoms will leave the trap for appropriate $\Delta\varphi$. Therefore, when measuring the ratio between the numbers of trapped atoms before and after the phase hop for different phase hop sizes, one can expect a clear signal from the experiment.

V. CONCLUSION

In conclusion we investigated the classical dynamics of a particle moving inside a rapidly oscillating potential

with a vanishing average. We found, that the motion of such a particle significantly depends on the oscillating potential's initial phase in the case that the particle is trapped. The well-known effective potential theory failed to describe this phenomenon and therefore needed to be extended. In agreement with the effective potential theory, we found that a particle moving inside a rapidly oscillating potential can be considered as though it was exposed to a time independent effective potential, however, this effective potential does not determine the particle's motion alone. Given the initial conditions of the particle, a transformation of these to effective initial conditions needs to be performed for which the effective potential then determines the correct motion of the particle. This transformation cannot be neglected even for arbitrarily high frequencies of the oscillating potential. It significantly depends on the initial phase of the oscillating potential and on the initial conditions of the particle itself. We could show that there always exist two initial phases of the oscillating potential such that the transformation can be neglected. Therefore, the effective potential theory in its previous form, which omits this transformation, can only describe these two special cases correctly. The phase dependence offers a new possibility to significantly manipulate the dynamics of a trapped particle. We explicitly calculated the change in a particle's period-averaged energy caused by a phase hop in the potential's modulation function. It is subject of future research to find applications of this novel tool of particle manipulation. The results presented in this article, should also be extended to the quantum regime.

ACKNOWLEDGMENTS

We would like to thank Shmuel Fishman, Roei Ozeri, Nir Bar-Gill, Rami Pugatch and Yoav Sagi for stimulating and inspiring discussions. This research was supported by the "Stiftung der Deutschen Wirtschaft" of the Federal Ministry of Education and Research (BMBF) of Germany and of the MINERVA Foundation.

-
- [1] P.L. Kapitza, *Zh. Eksp. Teor. Fiz.* **21**, 588 (1951).
 - [2] L.D. Landau and E.M. Lifschitz, *Mechanics* (Pergamon Press, Oxford, 1976).
 - [3] A.V. Gaponov and M.A. Miller, *Zh. Eksp. Teor. Fiz.* **34**, 242 (1958).
 - [4] H.G. Dehmelt, *Adv. At. Mol. Phys.* **3**, 53 (1967).
 - [5] I.C. Percival and D. Richards, *Introduction to Dynamics* (Cambridge University Press, London, 1982).
 - [6] B.B. Nadezhdin and E.A. Oks, *Pis'ma Zh. Tekh. Fiz.* **12**, 1237 (1986).
 - [7] M. Combescure, *Ann. Inst. Henri Poincaré A* **44**, 293 (1986).
 - [8] R.J. Cook, D.G. Shankland and A.L. Wells, *Phys. Rev. A* **31**, 564 (1985).
 - [9] T.P. Grozdanov and M.J. Raković, *Phys. Rev. A* **38**, 1739 (1988).
 - [10] S. Rahav, I. Gilary and S. Fishman, *Phys. Rev. Lett.* **91**, 110404 (2003); *Phys. Rev. A*, **68**, 013820 (2003).
 - [11] W. Paul, *Rev. Mod. Phys.* **62**, 531 (1990).
 - [12] R. Blatt, P. Gill and R.C. Thompson, *J. Mod. Opt.* **32**,

- 193 (1992).
- [13] J.I. Cirac and P. Zoller, *Phys. Rev. Lett.* **74**, 4091 (1995).
 - [14] D. Leibfried, R. Blatt, C. Monroe and D. Wineland, *Rev. Mod. Phys.* **75**, 281 (2003).
 - [15] F.G. Major, V.N. Gheorghe and G. Werth, *Charged Particle Traps: Physics and Techniques of Charged Particle Field Confinement* (Springer-Verlag, New York, 2004).
 - [16] N. Friedman, A. Kaplan, D. Carasso and N. Davidson, *Phys. Rev. Lett.* **86**, 1518 (2001).
 - [17] J.A. Sanders and F. Verhulst, *Averaging Methods in Non-linear Dynamical Systems* (Springer-Verlag, New York, 1985).